Eur Biophys J (2001) 30: 537–554
DOI 10.1007/s00249-001-0185-z

ARTICLE

**David A. Mannock · Ruthven N.A.H. Lewis
Ronald N. McElhaney · Paul E. Harper
David C. Turner · Sol M. Gruner**

An analysis of the relationship between fatty acid composition and the lamellar gel to liquid-crystalline and the lamellar to inverted nonlamellar phase transition temperatures of phosphatidylethanolamines and diacyl-α-D-glucosyl glycerols

Received: 6 June 2001 / Revised version: 3 September 2001 / Accepted: 3 September 2001 / Published online: 24 October 2001

Abstract The lamellar gel to lamellar liquid-crystalline (L_β/L_α) and lamellar liquid-crystalline to inverted hexagonal (L_α/H_{II}) phase transitions of a number of phosphatidylethanolamines (PEs) and diacyl-α-D-glucosyl-*sn*-glycerols (α-D-GlcDAGs) containing linear saturated, linear unsaturated, branched or alicyclic hydrocarbon chains of various lengths were examined by differential scanning calorimetry and low-angle X-ray diffraction. As reported previously, for each homologous series of PEs or α-D-GlcDAGs, the L_β/L_α phase transition temperatures (T_m) increase and the L_α/H_{II} phase transition temperatures (T_h) decrease with increases in hydrocarbon chain length. The T_m and the especially the T_h values for the PEs are higher than those of the corresponding α-D-GlcDAGs. For PEs having the same effective hydrocarbon chain length but different chain configurations, the T_m and T_h values vary markedly but with an almost constant temperature interval ($\Delta T_{L/NL}$) between the two phase transitions. Moreover, although the T_m and T_h values of the PEs and α-D-GlcDAGs are equally sensitive on the temperature scale to variations in the length and chemical configuration of the hydrocarbon chains, the $\Delta T_{L/NL}$ values are generally larger in the PEs and vary less with the hydrocarbon chain structure. This suggests that the PE headgroup has a greater ability to counteract variations in the packing properties of different hydrocarbon chain structures than does the α-D-GlcDAG headgroup. With decreasing chain length, this ability of the PE headgroup to counteract the hydrocarbon chain packing properties increases, significantly expanding the temperature interval over which the L_α phase is stable relative to the corresponding regions in the α-D-GlcDAGs. Overall, these findings indicate that the PEs have a smaller propensity to form the H_{II} phase than do the α-D-GlcDAGs with an identical fatty acid composition. In contrast to our previous report, there is some variation in the *d*-spacings of these various PEs (and α-D-GlcDAGs) in both the L_α and H_{II} phases when the hydrocarbon chain structure is changed while the effective chain length is kept constant. These hydrocarbon chain structural modifications produce different *d*-spacings in the L_α and H_{II} phases, but those changes are consistent between the PEs and α-D-GlcDAGs, probably reflecting differences in the hydrocarbon chain packing constraints in these two phases. Overall, our experimental observations can be rationalized to a first approximation by a simple lateral stress model in which the primary bilayer strain results from a mismatch between the actual and optimal headgroup areas and the primary strain in the H_{II} phase arises from a simple hydrocarbon chain packing term.

Keywords Differential scanning calorimetry · X-ray diffraction · Glucolipids · Phosphatidylethanolamines · Inverted hexagonal phase

D.A. Mannock · R.N.A.H. Lewis · R.N. McElhaney (✉)
Department of Biochemistry,
University of Alberta, Edmonton,
Alberta T6G 2H7, Canada
E-mail: rmcelhan@gpu.srv.ualberta.ca
Tel.: +1-780-4922413
Fax: +1-780-4920095

P.E. Harper[1] · D.C. Turner[2] · S.M. Gruner[3]
Department of Physics, Princeton University,
Princeton, NJ 05844, USA

Present addresses:
[1]Department of Physics and Astronomy,
Calvin College, 3201 Burton SE,
Grand Rapids, MI 49546, USA

[2]Vistakon, Johnson and Johnson Vison Care,
Inc., Mail Code R-R/D, PO Box 10157,
Jacksonville, FL 32247, USA

[3]Department of Physics, Cornell University,
Ithaca, NY 14853, USA

Abbreviations

DGDG: diglycosyl diacylglycerol
β-D-*GlcDAG*: 1,2-di-*O*-acyl-3-*O*-(*β*-D-glucopyranosyl)-*sn*-glycerol
α-D-*GlcDAG*: 1,2-di-*O*-acyl-3-*O*-(*α*-D-glucopyranosyl)-*sn*-glycerol
β-D-*GlcDAlkG*: 1,2-di-*O*-alkyl-3-*O*-(*β*-D-glucopyranosyl)-*sn*-glycerol
DSC: differential scanning calorimetry
ECL: equivalent chain length
H_{II}: inverted hexagonal
L_{α}: lamellar liquid-crystalline phase
L_{β}: lamellar gel phase
MGDG: monoglycosyl diacylglycerol
L/NL: lamellar/nonlamellar phase transition
PE: phosphatidylethanolamine
T_h: lamellar to inverted hexagonal phase transition temperature
T_m: chain-melting temperature of the lamellar gel phase
T_{NL}: lamellar to inverted nonlamellar phase transition temperature
$\Delta T_{L/NL}$: $T_{NL}-T_m$ (°C)
*18:1cΔ9-**: 1,2-di-*O*-[*cis*-9,10-octadecenoyl]-
18:1tΔ9-: 1,2-di-*O*-[*trans*-9, 10-octadecenoyl]-
$20{:}0_{eai}$-: 1,2-di-*O*-[16′-ethyl-octadecanoyl]-
$20{:}0_{dmi}$-: 1,2-di-*O*-[17′,17′-dimethyl-octadecanoyl]-
$19{:}0_{ai}$-: 1,2-di-*O*-[16′-methyl-octadecanoyl]-
$21{:}0_{ch}$-: 1,2-di-*O*-[15-cyclohexyl-pentadecanoyl]-
$19{:}0_{i}$-: 1,2-di-*O*-[17′-methyl-octadecanoyl]-
16:1tΔ9-: 1,2-di-*O*-[*trans*-9, 10-hexadecenoyl]-

* The numbers in the above abbreviated chemical nomenclature indicate the total number of carbon atoms in the hydrocarbon chain and the number (18:1), configuration (*cis* or *trans*) and position of any double bonds (Δ number) in the chain, whereas the subscripts (see below) indicate the type and position of the branches in the hydrocarbon chain (Lewis et al. 1989). Subscripts used in the above abbreviations: i: methyl-isobranched; ai: methyl-anteisobranched; ch: *ω*-cyclohexyl-branched; dmi: dimethyl-isobranched; eai: ethyl-anteisobranched.

Introduction

The monoglycosyl diacylglycerols (MGDGs) are important lipid components in the cell membranes of many prokaryotic microorganisms and plants (Ishizuka and Yamakawa 1985), where they seem to be the functional equivalents of the PEs present in the cell membranes of other prokaryotic microorganisms and eukaryotes. A characteristic feature of naturally occurring PEs and MGDGs is that they tend to form lamellar phases when dispersed in water at low temperatures, but inverted nonlamellar structures at elevated temperatures (Seddon et al. 1983, 1984, 1990; Jarrell et al. 1987; Mannock et al. 1988, 1990a, 1992; Lewis et al. 1989, 1990a, 1990b, 1994, 1997; Sen et al. 1990; Hinz et al. 1991; Mannock and McElhaney 1991; Lewis and McElhaney 1992, 1993; Turner et al. 1992; Trouard et al. 1994). The fact that almost all cell membranes contain significant quantities of "nonlamellar-forming lipids" has provided the impetus for a wide range of studies aimed at a definition of the functional roles of such lipids (Gruner 1992, 1994), as well as an understanding of the structural and physicochemical properties which predispose lipids to form such structures (Israelachvilli et al. 1977, 1980; Gruner 1985; Lewis et al. 1997).

The way in which a specific lipid chemical structure determines its phase preference is only partly understood. Israelachvilli et al. (1977, 1980) correlated lipid chemical structure and intermolecular interactions with the tendency of lipid molecules to form inverted, nonlamellar structures in terms of the probable "shape" of the lipid molecule. Alternatively, mesomorphs with curved lipid/water interfaces may be considered to be driven by a spontaneous curvature of the constituent lipid monolayers, with transitions between the lamellar and curved phases being driven by a competition between monolayer spontaneous curvature and stresses in the hydrocarbon chains in the curved phases (Kirk et al. 1984; Gruner 1985, 1992). Most of the data pertinent to such correlations have been obtained from studies of hydrated PEs and their analogues (Seddon et al. 1983, 1984; Lewis et al. 1989, 1997). Studies on such PEs indicate that the lamellar liquid-crystalline to inverted nonlamellar phase transition temperature (T_h) is sensitive to structural modifications in all regions of the PE molecule. Thus, for example, the T_h values of aqueous PE dispersions decrease with increasing hydrocarbon chain length (Lewis and McElhaney 1993), decrease when ester linkages between the hydrocarbon chains and the glycerol moiety are replaced with ether linkages (Seddon et al. 1983, 1984), but increase with structural modifications which increase the "size" of the polar headgroup or reduce its capacity to form hydrogen bonds (Gagne et al. 1985; Epand 1990; Trouard et al. 1994).

Changes in hydrocarbon chain structure also affect both the hydrocarbon chain-melting phase transition temperature (T_m) and the T_h of aqueous PE dispersions (Lewis et al. 1989, 1997). Our initial analysis of calorimetric measurements of PEs with comparable effective hydrocarbon chain lengths (ECLs)[1] showed that the difference between the T_m and the T_h remains relatively constant, irrespective of the temperatures at which their chain-melting transitions occur (Lewis et al. 1989).

[1]The effective chain length of a hydrocarbon chain is defined by the total number of carbons in the "main chain". For linear saturated and unsaturated fatty acyl chains, the effective chain length equals the total number of carbon atoms present, whereas for the branched fatty acyl chains the effective chain length equals that of the total number of carbon atoms minus those present in the branch(es). For *ω*-cyclohexyl fatty acyl chains, where three carbon atoms of the terminal six-membered ring actually form part of the main chain, the effective chain length is equal to the total number of carbon atoms present minus three

Interestingly, it was also found that, at the onset and completion temperatures of the L_α/H_{II} phase transition of PEs of comparable effective hydrocarbon chain lengths, the measured X-ray *d*-spacings were nearly independent of the chemical structure of the hydrocarbon chain. However, some of the structural dimensions presented in that earlier work (Lewis et al. 1989) were found to be incorrect, owing to ambiguity in the definition of "onset and completion temperatures" and faulty temperature calibration arising from a voltage bias in the temperature controller. The revised data now appear in a recently published report from our laboratories (Harper et al. 2001) and that new list of *d*-spacings at the L_α/H_{II} phase transition of those PEs is provided in Table 5 of this work for comparative purposes.

In order to further extend our initial analysis of the relationship between molecular structure and lipid nonlamellar propensity (Lewis et al. 1989), we have expanded our observations in two different directions. Firstly, a more substantial structural investigation of the 18-carbon ECL PEs was undertaken (Harper et al. 2001). Secondly, new calorimetric and low-angle X-ray diffraction measurements on two series of α-D-GlcDAGs containing 16-carbon and 18-carbon ECLs (both natural and synthetic) were performed, in order to investigate potential differences in the ability of the PE and MGDG headgroups to counteract the same hydrocarbon chain structural variations through changes in their thermotropic phase behaviour. In this new analysis, structural variations of the lipid hydrocarbon chains are evaluated in terms of variations in the T_{NL} and its proximity to the T_m. Such a comparison allows us to consider the differences in the chemical nature of the PE and α-D-Glc headgroups when attached to diacylglycerols containing a range of acyl chains (Harper et al. 1993, 2001; Lewis et al. 1997) in order to understand aspects of the molecular basis of the L/NL phase transition which cannot be addressed by studies of PE bilayers alone.

Materials and methods

With the exception of the 18:1*t*Δ9- and 16:1*t*Δ9-α-D-GlcDAGs, the glycolipids used in this study were synthesized from appropriate precursors using previously published methods (Mannock et al. 1990b). Details of the chemical structure of the hydrocarbon chains and lipid polar headgroups are shown in Fig. 1. Samples of 18:1*t*Δ9- and 16:1*t*Δ9-α-D-GlcDAG were purified from polar lipid extracts of *Acholeplasma laidlawii* B cultures which were made acyl chain homogeneous in 18:1*t* and 16:1*t* acids, respectively (Silvius and McElhaney 1978; Monck et al. 1992). Although we have successfully grown *A. laidlawii* B cultures on supplemented media with a range of methyl-iso-, methyl-anteiso- and dimethyl-isobranched fatty acids, it was easier to synthesize 100 mg batches of these α-D-GlcDAGs than to isolate them from cells because of the low yield (3–4 mg/L). This strategy also permitted the preparation of lipids containing fatty acids which resulted in either poor growth or no growth of *A. laidlawii* B cultures. The PEs are the same as those used in the recently published report by Harper et al. (2001) and were prepared as described by Lewis et al. (1989).

Samples were prepared for differential scanning calorimetry (DSC) as described by Mannock et al. (1990a) and were analyzed with a Perkin-Elmer DSC-2C scanning calorimeter equipped with a

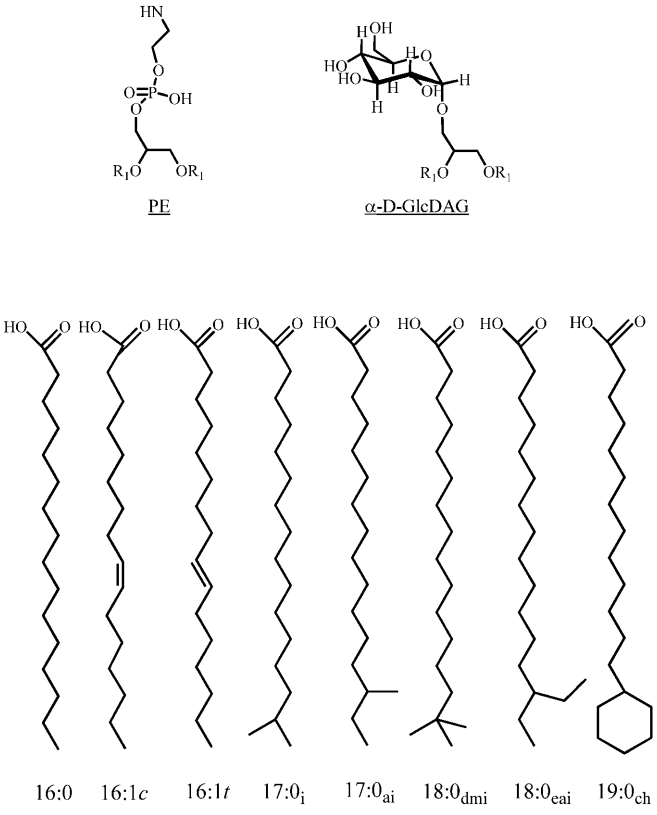

Fig. 1 Details of the lipid polar headgroup and hydrocarbon chain structures used in this study. The chain lengths shown are those of the 16-carbon ECL series. The 18-carbon ECL series are two carbons longer than those shown

PE-3700 thermal analysis data station. Duplicate samples were initially cycled between –3 and 97 °C at scan rates of up to 10 °C/min to ensure homogeneous hydration of the lipid. Once this protocol was completed, each sample was then rescanned up to four times at 1 °C/min in order to ensure that their thermotropic phase behaviour was repeatable. The minimum and maximum operating temperatures were selected and adjusted according to the observed chain melting and L/NL phase transition temperatures. For samples in which the above transitions fell above 10 °C and below 90 °C, the temperature limits were set at –3 and 97 °C. For samples in which the above phase transitions fell outside of this range, the boundary temperatures were changed incrementally in steps of 10 °C so that a flat baseline extending a minimum of 5 °C either below or above the respective transitions was observed. Where possible, this process was supported by reliable reports of the above phase transitions from the literature (Caffrey 1993; Marsh 1990). Data analysis was performed by importing the Perkin-Elmer-DSC-2 data files into Microcal Origin software (Microcal, Northampton, Mass.). The slope and curvature of the rough data were corrected by baseline subtraction and the phase transition temperatures measured from the peak maximum.

Many of the glycolipids investigated here form L_β (or L_β') gel phases which are unstable at temperatures below the T_m, and, once cooled to such temperatures, the nucleation and growth of "stable" lamellar crystalline (L_c) forms of the lipid occur. It is often the case that the transition temperature of the L_c phase of the lipid is higher than the T_m and with some lipids it may even be higher than the T_{NL}. Thus, depending upon the kinetics of the process, DSC heating thermograms of such lipids can be very complex and the metastable L_β/L_α and sometimes the lamellar/H_{II} endothermic transitions of the lipid may be obscured by thermal events arising from the formation or the melting transitions of the crystalline polymorphs. In order to overcome this problem, some lipid

samples were cooled to a temperature just below the T_m and were then reheated before the L_c phase could reform. In our experience, this protocol does not introduce thermal artifacts when the nucleation temperature of the L_c phase is not close to the T_m. By using this approach, the transition temperatures of poorly energetic thermal events can be measured in an accurate and repeatable manner. This protocol allowed us to investigate the metastable phase behaviour of this collection of lipids and was also a useful aid in identifying the L_α/H_{II} phase transition which, at slow scan rates, only differed by about 2 °C between heating and cooling measurements.

The preparation of the PE and α-D-GlcDAG samples and the small-angle X-ray methods are the same as those described in Lewis et al. (1989). Briefly, X-rays were generated on a rotating anode X-ray generator. The beam line was equipped with single-mirror Franks optics, a thermostated (–30 to 100 °C) specimen stage, and an area X-ray detector. The area detector was either the area detector described in Reynolds et al. (1978) or the successor detector in which the silicon diode vidicon camera was replaced with a slow-scan CCD camera (the "intensifier/lens/CCD" camera described in Tate et al. 1997). In what follows, "*d*-spacing" refers to the unit cell basis vector length. Determinations of the phase behavior and structural dimensions of some of the PEs are described in Harper et al. (2001). A detailed Fourier reconstruction of the glycolipids has not been undertaken at this time (see Discussion) and a complete thermodynamic and structural overview of both the 16- and 18-carbon ECL glycolipids will follow (D. Mannock et al., manuscript in preparation).

Results

Calorimetry

DSC was used to obtain accurate measurements of the L_β/L_α and L_α/H_{II} phase transition temperatures (T_m and T_h values, respectively) of a wide range of α-D-GlcDAGs, and X-ray diffraction was used to measure the *d*-spacings of the lamellar and the inverted nonlamellar phases of each lipid as a function of temperature and to assign phase structures above and below the phase transitions reported by DSC.

DSC thermograms of a representative glycolipid, $20{:}0_{dmi}$-α-D-GlcDAG, are shown in Fig. 2a. The heating thermogram (lower trace) contains three endothermic events centred at 35.0, 38.6 and 56.4 °C, which are reversible on cooling (upper trace). The two highly energetic components seen on heating between 30 and 40 °C correspond to an L_c/L_β phase transition followed by an L_β/L_α phase transition, whereas the less energetic event at 56.4 °C marks the L_α/H_{II} phase transition. These phase transition temperatures and phase assignments were confirmed by the low-angle X-ray diffraction measurements.

Effects of hydrocarbon chain length on T_m and T_{NL}

The T_m and T_{NL} values obtained from our DSC measurements of 16- and 18-carbon ECL PEs and α-D-GlcDAGs are listed in Tables 1 and 2. These data and that obtained from similar measurements of the diacyl PEs, the 1,2-*O*-diacyl-3-*O*-(β-D-galactopyranosyl)- and (β-D-glucopyranosyl)-*sn*-glycerols (Mannock et al. 1988, 2000, 2001), which outline the metastable phase behavior for each headgroup variant, are summarized in Fig. 3.

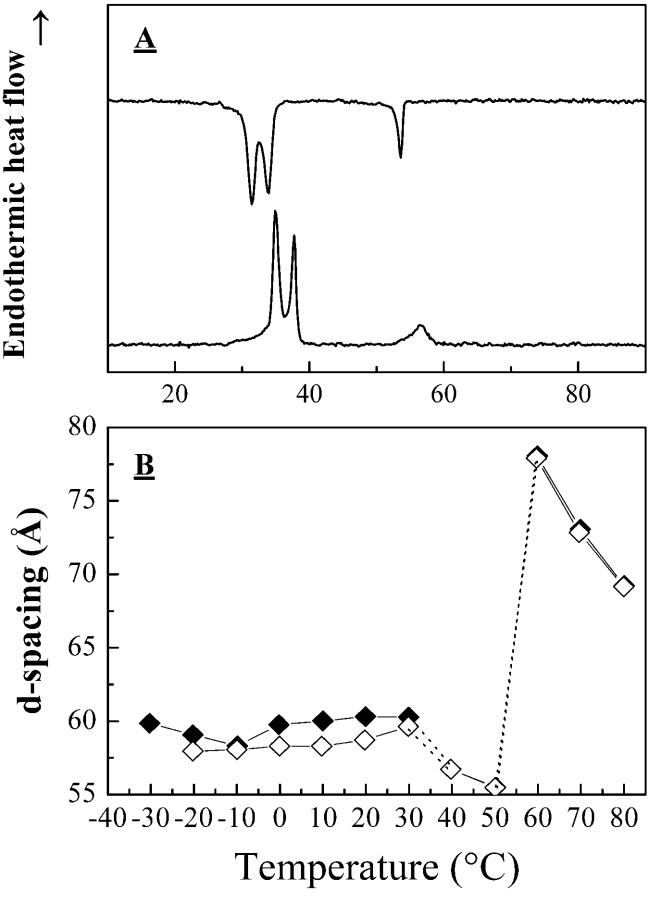

Fig. 2 **A** Typical heating and cooling DSC thermograms of $20{:}0_{eai}$-α-D-GlcDAG obtained at 1 °C/min. The heating scan is the *lower curve* and the cooling scan is the *upper curve*. **B** A plot of the X-ray diffraction *d*-spacings for $20{:}0_{eai}$-α-D-GlcDAG as a function of temperature. The *filled symbols* were collected in the heating direction and the *empty symbols* were collected in the cooling direction. The *dotted lines* indicate a temperature range over which a phase transition was observed. The data for this glycolipid sample were collected every 10 °C

Typically, for any given homologous lipid series, the T_m increases with increasing hydrocarbon chain length but with progressively smaller increments per additional methylene unit. Figure 3 clearly shows that this behaviour is common to all headgroup variants. Thus, for a given series of lipids, the transition temperatures between the lamellar gel phase and all liquid-crystalline phases (lamellar or nonlamellar) describe a type of "saturation" curve, which is presumed to approach a limiting value at infinite hydrocarbon chain length (Fig. 3). Linear transformations of the data along the lines proposed by others (Nagle and Wilkinson 1978; Marsh 1991) suggest that, upon extrapolation of these glycolipid T_m values to infinite hydrocarbon chain length, all the curves should converge in a temperature range near to the melting point of polyethylene, independent of the headgroup.

Table 1 The effect of hydrocarbon chain length on the calorimetrically determined phase transition temperatures (°C) of monoglycosyl diacylglycerols

Chain length	T (°C) (L_β/L_α)	T (°C) (L_β/H_{II})	T (°C) (L_α/Q_{II})	T (°C) (L_α/H_{II})	T (°C) (Q_{II}/H_{II})	T (°C) $\Delta T_{L/NL}$	Ref
n-Saturated α-D-glucosyl diacylglycerols (1,2-*sn*)							
12	19.5	–	–	–	–	–	c
13	32.9	–	–	–	–	–	c
14	40.5	–	105.0[a]	–	–-	64.5	c
15	50.7	–	82.0[a]	–	–	31.3	c
16	57.2	–	79.1[a]	–	119.0	21.9	c
		–	–	–	–	61.8	c
17	63.4	–	–	76.6	–	13.2	c
18	68.4	–	–	74.5	–	6.1	c
19	–	73.7	–	–	–	–	c
20	–	76.8	–	–	–	–	c
n-Saturated α-D-glucosyl di-isoacylglycerols (1,2-*sn*)							
14_i	0.46	–	70.2[a]	–	–	69.7	d
15_i	3.0	–	69.3[a]	–	–	66.3	d
16_i	25.1	–	–	67.9	–	25.1	d
17_i	34.5[b]	–	–	67.9	–	33.4	d
18_i	44.5	–	–	67.7	–	23.2	d
19_i	51.0	–	–	69.0	–	18.0	d
20_i	57.7	–	–	68.1	–	10.6	d

[a]Cubic phase
[b]Some 16-ECL-MGDGs exhibit L_α/Q_{II} phase coexistence on cooling
[c]Mannock et al. (1990a)
[d]Mannock et al. (unpublished data)

Table 2 The effect of hydrocarbon chain length on the calorimetrically determined phase transition temperatures (°C) of diacylphosphatidylethanolamines

Chainlength	T (°C) (L_β/L_α)	T (°C) (L_α/H_{II})	T (°C) $\Delta T_{L/NL}$	Ref
n-Saturated diacylphosphatidylethanolamines (1,2-*sn*)				
10	2.0	–	–	a–c
11	16.9	–	–	a–c
12	31.3	–	–	a–c
13	42.1	–	–	a–c
14	50.4	–	–	a–c
15	58.4	–	–	a–c
16	64.4	118.5	54.1	a–c
17	70.5	107.6	37.1	a–c
18	74.2	99.2	25.0	a–c
19	79.2	98.0	18.8	a–c
20	83.4	97.2	13.8	a–c
n-Saturated di-isoacylphosphatidylethanolamines (1,2-*sn*)				
17_i	42.3	104.0	67.1	b
18_i	52.0	94.0	44.0	b
19_i	59.0	88.0	29.0	b
20_i	64.0	86.5	21.5	b

[a]Lewis and McElhaney (1993)
[b]Lewis et al. (1989)
[c]Seddon et al. (1983)

Although the T_m values of these lipids vary smoothly as a function of hydrocarbon chain length, the type of phase transition which occurs at the T_m is chain length dependent (Fig. 3). With the shorter-chain members of any MGDG homologous series, the process which occurs at the T_m is the L_β/L_α phase transition which, typically, is very energetic, highly cooperative and thermally reversible with little or no hysteresis upon cooling. With the longer chain lipids, the H_{II} phase is the only stable liquid-crystalline phase observed and, at the T_m, the L_β phase converts directly to the H_{II} phase via a very energetic and highly cooperative phase transition (Fig. 3). Interestingly, there does not appear to be any discontinuity in the curve describing the chain length dependence of the T_m, despite the differing nature of the phase transitions that occur at longer chain lengths. However, a discontinuity in the thermodynamic parameters is most often observed in the chain length

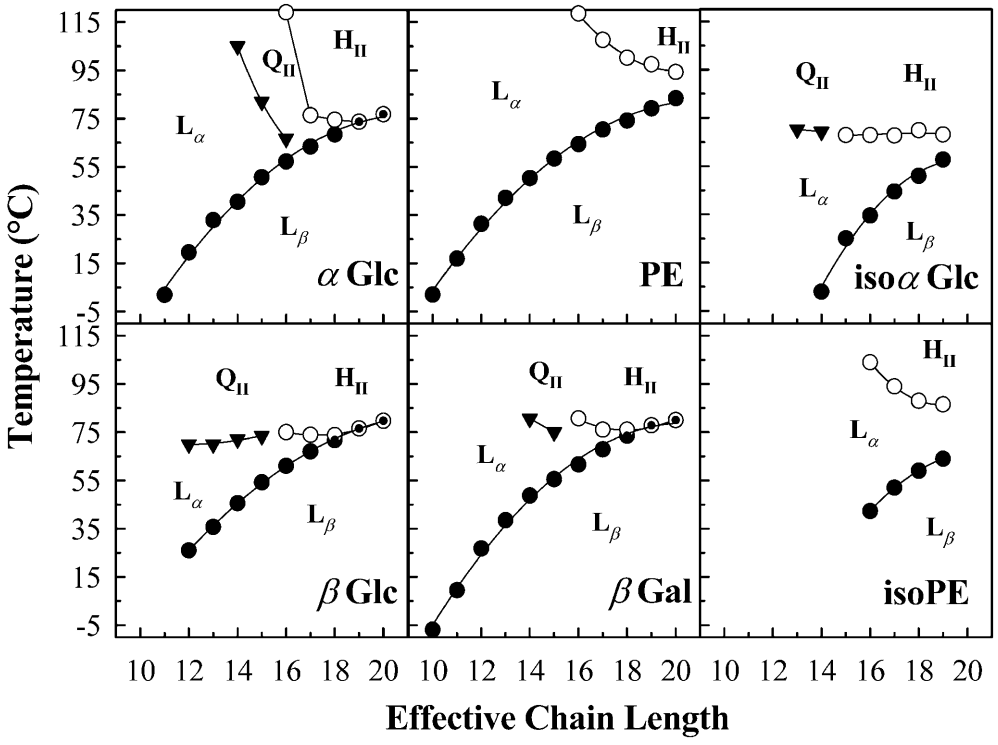

Fig. 3 Plots of the phase transition temperatures observed by DSC of a selection of phosphatidylethanolamines and D-glycosyl diacylglycerols with different headgroup and hydrocarbon chain structures. The symbols are as follows: *filled circles*: chain-melting phase transitions from the L_β phase; *empty circles*: transitions to the H_{II} phase; *filled inverted triangles*: L_α/Q_{II} phase transitions. The data are from the following sources: di-saturated-α-D-Glc-DAGs (Mannock et al. 1990a), di-saturated-β-D-GlcDAGs (Mannock et al. 1988), di-saturated-β-D-GalDAGs (Mannock and McElhaney 1991; Mannock et al. 2001), methyl-iso-branched-α-D-GlcDAGs (Lewis et al. 1990a, 1997; D. Mannock unpublished results), di-saturated PEs (Lewis and McElhaney 1993), methyl-iso-branched PEs (Lewis et al. 1989, 1997)

Table 3 The effect of hydrocarbon chain structure on the calorimetrically determined phase transition temperatures (°C) of 1,2-di-*O*-acyl-3-*O*-(α-D-glucopyranosyl)-*sn*-glycerols

Chainstructure	T (°C) (L_β/L_α)	T (°C) (L_α/Q_{II})	T (°C) (L_α/H_{II})	T (°C) (Q_{II}/H_{II})	T (°C) $\Delta T_{L/NL}$	Ref
Equivalent chain length: 16 carbon atoms						
16:0	57.2	79.1[a]	–	119.0	21.8	c
16:1$t\Delta$9	12.0	38.0[a]	–	64.0	26.0, 52.0	d
18:0_{eai}	−13.3	–	33.1	–	46.4	d
18:0_{dmi}	18.3	–	52.0	–	33.7	d
17:0_{ai}	16.2	–[b]	56.6	–	40.4	d
17:0_{i}	34.5	–[b]	67.9	–	33.4	d
19:0_{ch}	28.5	–	60.8	–	32.3	d
Equivalent chain length: 18 carbon atoms						
18:0	68.4	–	74.5	–	6.1	c
18:1$t\Delta$9	29.3	–	34.0	–	4.7	e
20:0_{eai}	6.5	–	30.5	–	24.0	e
20:0_{dmi}	38.6	–	56.4	–	17.8	e
19:0_{ai}	35.3	–	60.5	–	25.2	e
19:0_{i}	51.0	–	69.0	–	18.0	e
21:0_{ch}	45.8	–	63.6	–	17.8	e

[a]The di-16:1*t*-MGDGs form an intermediate Q_{II} phase on heating and cooling
[b]Some 16-ECL-MGDGs exhibit L_α/Q_{II} phase coexistence on cooling
[c]Mannock et al. (1990a)
[d]Mannock et al. (unpublished data)
[e]Lewis et al. (1990a)

dependence of the enthalpy values of a homologous series as the L_β/L_α and L_α/H_{II} phase transitions become one event (Lewis and McElhaney 1993; Lewis et al. 1994; Mannock et al. 2000). This may simply be a reflection of the fact that the T_m is primarily determined by the thermodynamic stability of the gel phase.

At temperatures above the T_m, the L_α phases of the shorter chain MGDG homologues become unstable with respect to one or more inverted cubic phases and thermotropic events corresponding to L_α/Q_{II} phase transitions are observed. Typically, the L_α/Q_{II} transitions of these lipids are weakly energetic and poorly cooperative processes which often exhibit considerable hysteresis upon cooling. At first glance, our results suggest that the L_α/Q_{II} phase transition temperatures of the MGDGs studied here exhibit a relatively weak chain length dependence. However, in compounds with a weak L_α/Q_{II} phase transition temperature chain length

Table 4 The effect of hydrocarbon chain structure on the calorimetrically determined phase transition temperatures (°C) of phosphatidylethanolamines

Chain structure	T (°C) (L_β/L_α)	T (°C) (L_α/Q_{II})	T (°C) (L_α/H_{II})	T (°C) (Q_{II}/H_{II})	T (°C) $\Delta T_{L/NL}$	Ref
Equivalent chain length: 18 carbon atoms						
18:0	74.2	–	99.2	–	25.0	a–c
18:1*c*Δ9	–16.0	–	10.0	–	26.0	d
18:1*t*Δ9	37.4	–	65.0	–	27.6	e
$20{:}0_{eai}$	24.0	–	52.0	–	28.0	b
$20{:}0_{dmi}$	43.2	–	74.0	–	30.8	b
$19{:}0_{ai}$	44.6	–	80.5	–	35.9	b
$19{:}0_{i}$	59.0	–	88.0	–	29.0	b
$21{:}0_{ch}$	54.0	–	82.8	–	28.8	b
18:1*cc*Δ9,12	–40.0	–	–15.0	–	25.0	f

[a]Lewis and McElhaney (1993)
[b]Lewis et al. (1989)
[c]Seddon et al. (1983)
[d]Cullis and de Kruijff (1978)
[e]Epand (1990)
[f]Dekker et al. (1983)

dependence, more than one cubic phase structure is often observed with increasing temperature by X-ray diffraction (usually with *Ia*3*d* and *Pn*3*m* symmetry). In the saturated straight-chain α-D-GlcDAGs, where the dominant Q_{II} phase has *Ia*3*d* symmetry at all temperatures measured, a strong chain length dependence of the L_α/Q_{II} phase transition temperature is observed (Fig. 3). These differences in the pattern of Q_{II} phase behaviour probably originate from small differences in the curvature free energy between these two Q_{II} phases and from other factors such as headgroup and interfacial hydration (Turner et al. 1992; Templer et al. 1995).

Upon heating these shorter chain glycolipids to higher temperatures, the Q_{II} phases undergo Q_{II}/H_{II} phase transitions. This sequence of phase transitions can only be inferred at very short chain lengths, where the required temperature range is above the recommended safety limit for the analysis of hydrated samples in our DSC instrument. Where Q_{II}/H_{II} phase transitions are observed, they are weakly energetic and poorly cooperative processes, but, unlike the L_α/Q_{II} phase transitions, are freely reversible and exhibit little or no cooling hysteresis.

In the medium chain MGDG homologues, L_β/L_α phase transitions are clearly delimited at lower temperatures. However, when heated to higher temperatures, Q_{II} phases are not normally observed in these samples and the L_α phase converts directly to the H_{II} phase. With these lipids, the L_α/H_{II} phase transitions are weakly energetic but fairly cooperative processes which exhibit only a modest cooling hysteresis (typically < 3 °C). The L_α/H_{II} transition temperatures also decrease with increasing chain length but at rates which are considerably smaller than those which typify the chain length dependence of the Q_{II}/H_{II} transitions of the shorter chain homologues. In this range of hydrocarbon chain lengths there tends to be a relatively small temperature window over which the L_α phase is observed. This window becomes progressively smaller and vanishes when the curves defining the L_α/H_{II} and L_β/L_α phase boundaries intersect, at which point only a single L_β/H_{II} phase transition is observed (Fig. 3). For the purposes of this study, the intersection of these two curves will be considered as an arbitrary boundary between the medium chain and long chain members of a homologous series.

At short chain lengths, the saturated straight-chain PEs and their methyl-isobranched counterparts are lamellar and show no evidence of forming cubic phases over the temperature ranges examined in our studies (Lewis et al. 1989 and references cited therein). With increasing chain length in the above-mentioned PEs, the L_α/H_{II} phase transition, which is initially seen at much higher temperatures than in the glycolipids of equal chain length, shifts to lower temperatures. However, the pattern of separate L_β/L_α and L_α/H_{II} phase transitions is not replaced by a single L_β/H_{II} phase transition at the longest ECLs examined in our studies (Lewis et al. 1989) in either the straight chain or isobranched PEs.

Effects of hydrocarbon chain structure on T_m and T_{NL}

The effect of hydrocarbon chain structure was evaluated by a comparative study of various α-D-GlcDAGs and PEs of similar ECLs but containing different hydrocarbon chain structures. The results of parallel studies of glucolipids of ECLs equivalent to linear chains consisting of 16- and 18-carbon atoms are shown in Table 3. The dominant feature of the data presented is that, for any effective chain length, modification of the *n*-saturated hydrocarbon chain structure, whether by branching or by the introduction of a double bond, results in a lowering of both the T_m and T_{NL}. Irrespective of hydrocarbon chain length, both the T_m and T_{NL} values of this group of MGDGs decrease in the following order: linear saturated > methyl-iso > ω-cyclohexyl > dimethyl-iso≈methyl-anteiso > *trans*-monounsaturated > ethyl-anteiso > *cis*-unsaturated > *cis*-diunsaturated. Both transition temperatures become progressively lower as the size of substituent groups at the hydrophobic termini of the chains increases ($18{:}0 > 18{:}0_i > 21{:}0_{ch}$), as the

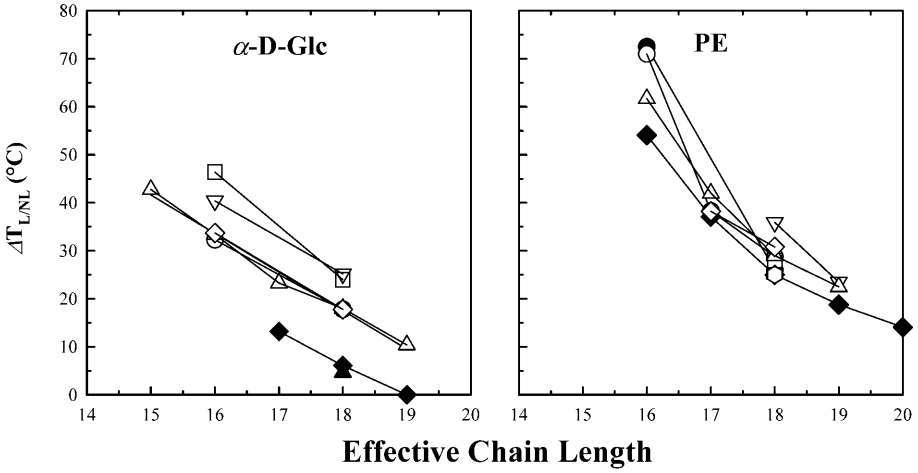

Fig. 4 Plots of $\Delta T_{L/NL}$ for both the α-D-GlcDAGs and the corresponding PEs as a function of effective chain length. References to the original work appear in the legend to Fig. 3. The symbols for each lipid are as follows: *filled circles*: di-*cis*-monounsaturated; *filled triangles*: di-*trans*-monounsaturated; *empty squares*: ethyl-anteiso-branched; *empty diamonds*: dimethyl-iso-branched; *empty triangles*: methyl-iso-branched; *inverted empty triangles*: methyl-anteiso-branched; *empty circles*: ω-cyclohexyl-branched; *filled circles*: di-saturated; *empty hexagon*: di-*cis*-diunsaturated

number of substituents at any given position increases ($18{:}0 > 19{:}0_{ai} > 20{:}0_{dmi}$), or as the position of the substituent is moved towards the centre of the chain ($19{:}0_{i} > 19{:}0_{ai}$). A similar pattern of behavior was observed in our previous studies of aqueous PE dispersions, as seen in Table 4 (Lewis et al. 1989).

The other interesting feature of the glycolipid data presented in Tables 3 and 4 is the relationship between hydrocarbon chain structure, hydrocarbon chain length and T_{NL}. With the linear saturated and *trans*-monounsaturated lipids, the T_{NL} of the 16-carbon species is lower than that of the 18-carbon homologue. This observation is contrary to expectations, since the tendency to form a nonlamellar phase should increase with increasing hydrocarbon chain length, as seen in comparable studies of hydrated PEs (Lewis et al. 1989). The reason that this behaviour is observed with the MGDGs but not the PEs is the existence of multiple nonlamellar phases in the shorter-chain members of the former compounds. The di-isoacyl-α-D-glucolipids (D. Mannock et al. unpublished data) are good examples of this behaviour, since T_{NL} is almost chain length invariant over the entire range of chain lengths studied, primarily because the nature of the nonlamellar phase changes from Q_{II} to H_{II} with increasing chain length (see Tables 1 and 2). This also explains why the T_{NL} values of the 18-carbon homologues for a number of the other branched-chain lipids are higher than those of the corresponding 16-carbon homologues in the α-D-GlcDAGs (Table 3) but not the PEs, where the H_{II} phase is the only thermodynamically stable nonlamellar phase observed.

We also find that the difference between the T_m and T_{NL} values (i.e., the temperature interval between the melting of the hydrocarbon chains to the formation of the nonlamellar phase, $\Delta T_{L/NL}$) of the 18-carbon ECL α-D-GlcDAGs is always smaller than that observed in their 16-carbon homologues (Fig. 4). In addition to the chain length dependence of $\Delta T_{L/NL}$, there are indications from the progression of the $\Delta T_{L/NL}$ parameter in the 18-carbon ECL lipids in Fig. 4 that there is also a dependence on chain structure in both lipid series. Closer inspection of the data for both the PEs and α-D-GlcDAGs shows that the $\Delta T_{L/NL}$ values of the linear saturated and *trans*-monounsaturated lipids occur at the low end of the range observed for this parameter. In particular, in the 18 ECL glucolipids, the $\Delta T_{L/NL}$ values of the 18:0 and 18:1*t*Δ9 compounds differ from those of the corresponding branched-chain lipids by approximately 15 °C. The corresponding data for the α-D-GlcDAGs and PEs differ from one another in the range of their $\Delta T_{L/NL}$ values at a specific chain length (at 18-carbon ECL the α-D-GlcDAGs range from ~5 to 25 °C, whereas the corresponding PEs range from ~25 to 35 °C), suggesting that the PE headgroup has a greater stabilizing effect on the lamellar phase with differences in chain structure than does the glycolipid headgroup (Fig. 3; Lewis et al. 1989).

X-ray diffraction measurements

Initial studies of the diacyl-α-D-GlcDAGs using small-angle X-ray diffraction confirmed the phase transition temperatures seen by DSC (Fig. 2a) and the diffraction patterns obtained allowed the unambiguous differentiation of the lamellar, Q_{II} and H_{II} phases present (Fig. 5). An X-ray diffraction temperature profile for a representative α-D-GlcDAG is shown in Fig. 2b. The temperature dependence of the *d*-spacings clearly shows that the phase behaviour seen on heating is reversible on cooling. At lower temperatures between –40 and 30 °C, a lamellar phase is observed with a *d*-spacing of 60.3 Å. Continued heating to above 40 °C shows a transition to a lamellar liquid crystalline phase (55.5 Å), which then converts to a H_{II} phase at about 55 °C (78.1 Å). Representative diffraction profiles of the L_α and H_{II} phases from the 20_{dmi}-α-D-GlcDAG and a Q_{II} phase diffraction pattern from the di-16:1*t*-α-D-GlcDAG are shown in Fig. 5. Discontinuities in the X-ray spacings provided confirmation of the lamellar/nonlamellar phase transition temperatures in both the PEs and the α-D-GlcDAGs (see Table 5 and later section). An analysis of the

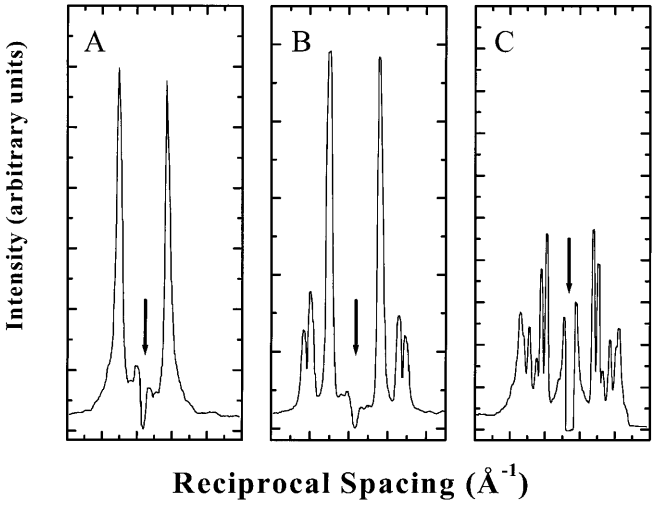

Fig. 5 Representative X-ray diffraction patterns for **A** the L_α phase at 50 °C, **B** the H_{II} phase at 60 °C of 20:0_{eai}-α-D-GlcDAG and **C** the Q_{II} phase at 40.4 °C of 16:1*t*Δ9-α-D-GlcDAG

small-angle X-ray diffraction patterns allowed the unambiguous differentiation between L_α/Q_{II}, Q_{II}/H_{II} and L_α/H_{II} phase transitions.

The effects of changes in hydrocarbon chain length and structure in these glycolipids were also examined by comparison of the X-ray *d*-spacings at the phase transition temperature of the L_α/H_{II} phase transition of these lipids. In general, the *d*-spacing at the phase transition was determined by making a linear fit of the *d*-spacings as a function of temperature for a given phase and then evaluating the fit at the phase transition temperature determined by the DSC work. In the case of 18:1*c*Δ9-PE in the hexagonal phase, a quadratic fit was used. This comparison was prompted by previous studies of an analogous series of diacyl PEs (Lewis et al. 1989), where we observed that these values were similar regardless of hydrocarbon chain structure[2]. The measurements obtained for *d*-spacings at the L_α/H_{II} phase transitions of the 16- and 18-carbon α-D-GlcDAGs, as well as those of the corresponding PEs (Harper et al. 2001), are summarized in Table 5. The PE data in Table 5 (from Harper et al. 2001) are more accurate than the data we presented in Lewis et al. (1989). The diffraction data were acquired by changing the sample temperature in discrete steps and, after a short equilibration time at each temperature, acquiring a new diffraction pattern. The temperature interval between diffraction patterns limits the precision with which one can use diffraction data to assign the onset and completion of a phase transition. This is especially problematic with L/NL transitions since, in practice, phase coexistence is seen over a span of many degrees (e.g., see Tate et al. 1992). Lewis et al. (1989) used steps as large as 10 °C. It was also discovered that the temperature calibration of the specimen stage was in error by a few degrees. Harper et al. (2001) re-examined the diacyl PEs studied by Lewis et al. (1989) but with finer temperature steps and improved calibrations. From these improved data we conclude that the unit cell basis vector lengths (i.e., the *d*-spacings) on either side of the L_α/H_{II} are generally similar for all the diacyl PEs studied, although the more accurate data shows considerably more spread than was reported in Lewis et al. (1989).

Increasing the hydrocarbon chain length by the insertion of additional methylene units is known to produce a relative increase in the *d*-spacings of the L_α and H_{II} phases in the α-D-GlcDAGs and PEs (Sen et al. 1990; Lewis et al. 1989). The effect of changes in the hydrocarbon chain structure of these lipids on the *d*-spacings of both the L_α and H_{II} phases on both the normal and reduced temperature scales (defined as T–T_h) are shown in Fig. 6. On the reduced temperature scale, the *d*-spacings of all lipids in the L_α phase at a given temperature are spread over a range of bilayer thickness, but appear to follow a generally similar order. However, this order is not well correlated with the phase transition temperature measurements of the α-D-GlcDAGs and PEs. The *d*-spacings in the H_{II} phase show a much greater range of values at a given temperature. In the PEs the order of the *d*-spacings is similar in both the L_α and H_{II} phases, except for lipids containing an ω-cyclohexyl-terminated acyl chain, which is known to have atypical motional and packing properties (see Discussion). In the 16- and 18-ECL α-D-GlcDAGs, the dependence of the L_α and H_{II} d-spacings on chain structure follow the same general trend, but shows minor differences in order between the phases and when compared with the corresponding measurements in the PEs. This suggests that the changes in hydrocarbon chain length and structure have a similar effect on the lipid phase behaviour despite differences in headgroup structure. The question that remains unanswered is which portion of the lipid molecule is driving the L_α/H_{II} phase transition (see Discussion).

Discussion

Calorimetry

An understanding of lipid phase transitions involves knowledge of the way in which local lipid-lipid and lipid-water interactions give rise to the component forces that are ultimately responsible for the molecular packing and phase behaviour. These phase properties can be considered in terms of the sum of all molecular interactions from three single regions: the hydrocarbon chains, the interfacial region and the lipid polar headgroup. Such boundaries cannot be strictly delimited, because each

[2]In Lewis et al. (1989), a table of "onset and completion" *d*-spacings was constructed. Unfortunately, the idea of "onset and completion" is functionally ambiguous, as phase coexistence is seen over a span of many degrees and the X-ray diffraction data were taken in discrete steps as large as 10 °C. Hence, the "onset and completion" *d*-spacings end up being dependent on the temperature step size used

Table 5 The structural data obtained for the phosphatidylethanolamines (*d*-spacing, *w*, *r*, $<l>$ and *A*, all in Å) and α-D-glucosyl diacylglycerols (*d*-spacing, Å) at the lamellar liquid-crystalline to inverted hexagonal phase transition

Diacyl-PE[a]	ECL = 18 carbons[b]			Additional PE structural parameters					
	$T_{L/NL}$ (°C)	*d*-spacing		L_α phase (Å)			H_{II} phase (Å)		
Chain structure		L_α (Å)	H_{II} (Å)	*w*	$<l>$	*A*	*r*	$<l>$	*A*
cis-Monounsat	10.0	52.1	77.9	12.8	19.7	61.0	22.9	17.6	47.7
trans-Monounsat	65.0	51.6	75.0	12.5	19.5	62.8	20.9	18.2	46.1
Ethyl-aiso	52.0	56.3	84.2	13.1	21.6	62.8	23.1	20.9	44.1
Dimethyl-iso	74.0	55.9	82.7	12.3	21.8	64.2	22.7	20.5	46.2
Methyl-aiso	80.5	54.0	78.6	12.2	20.9	64.1	21.5	19.6	46.3
Methyl-iso	88.0	54.4	79.1	12.2	21.1	64.2	21.7	19.7	46.7
ω-Cyclohexyl	82.8	56.3	80.5	12.4	21.9	63.5	21.6	20.5	45.7

α-D-GlcDAG	ECL = 16 carbons			ECL = 18 carbons[b]		
		d-spacing			*d*-spacing	
Chain structure	$T_{L/NL}$ (°C)	L_α (Å)	H_{II} (Å)	$T_{L/NL}$ (°C)	L_α (Å)	H_{II} (Å)
n-Sat'd		–	–	74.5	54.1	71.5
trans-Monounsat	38.0[c]	47.8	63.0	34.0	51.0	73.0
Ethyl-aiso	33.1	51.0	79.0	30.5	56.5	82.0[e]
Dimethyl-iso	52.0	52.0	76.0	56.4	55.0	79.0
Methyl-aiso	56.6[d]	50.0	71.0	60.5	53.0	72.0
Methyl-iso	67.9[d]	51.0	73.0	69.0	56.0	77.0
ω-Cyclohexyl	60.8	53.0	70.0	63.6	57.0	74.0

[a]Harper et al. (2001)

[b]The *d*-spacings for the 18-carbon saturated and monounsaturated lipids appear slightly smaller than those of the branched chain lipids in both the lamellar and nonlamellar phases. The PEs have errors of ±0.5 Å, whereas the glycolipids have errors of ±1–2 Å. Refer to the text for the method of determining the *d*-spacing at the phase transition

[c]The di-16:1*t*-MGDGs forms an intermediate Q_{II} phase on heating and cooling

[d]Some 16-ECL-MGDGs exhibit L_α/Q_{II} phase coexistence on cooling

[e]The *d*-spacing data for 18-ethyl-aiso-MGDG in the H_{II} phase exhibits a kink close to the L_α/H_{II} phase transition. Therefore, it was not possible to produce a smooth line that fitted the data exactly, as was done for the other data sets. Instead, we list a H_{II} phase *d*-spacing measured experimentally at a temperature close to the phase transition

region is not isolated from the other and thus there must be interaction throughout the entire lipid molecule. Nevertheless, such delineation provides a convenient means for comparisons that give insight into the effects of structural changes on lipid phase properties. Since we did not vary the glycerol-hydrocarbon chain linkage in this study (both the PEs and the α-D-GlcDAGs have diacylglycerol backbones), our data is interpreted in terms of the contributions from changes in the hydrocarbon chain length and structure, and from changes in the polar headgroup structure.

Hydrocarbon chain length and structure

Increasing the length of the hydrocarbon chains in saturated straight-chain glycerolipids increases the T_m and decreases the T_h. Almost any structural modification of the linear, saturated hydrocarbon chain (other than chain length) causes a relative decrease in both the T_m and the T_h. In most cases, modification of the hydrocarbon chain structure destabilizes the gel phase hydrocarbon chain packing relative to that of the linear, saturated hydrocarbon chain (see Tables 3 and 4). However, the presence of substituent groups that decrease the tightness of lipid hydrocarbon chain packing in the gel state, thus decreasing T_m, also restricts the conformational freedom of the hydrocarbon chains in the liquid-crystalline state, at least on the reduced temperature scale. Thus, the cross-sectional areas occupied by monolayers of synthetic PCs and synthetic α-D-GlcDAGs of comparable ECLs at the air-water interface decrease in the liquid-expanded state in the order: linear saturated > methyl-iso- > methyl-anteiso- > ω-cyclohexyl-branched, when compared at equivalent temperatures above their liquid-condensed/liquid-expanded phase transition temperatures (Rice et al. 1987; Balthasar et al. 1988; Ashgarian et al. 1989, 2000). The area occupied per molecule increases with increasing hydrocarbon chain length at comparable reduced temperatures within each of these four series of synthetic PCs (Rice et al. 1987; Balthasar et al. 1988; Ashgarian et al. 1989). Similarly, the chain-averaged orientational order of the lipids of the *Acholeplasma laidlawii* membrane decrease in the order: *cis*-monounsaturated > *trans*-monounsaturated > methyl-anteiso-branched > methyl-iso-branched > linear saturated when compared in the liquid-crystalline state at comparable reduced temperatures above the gel/liquid-crystalline phase transition temperature (Macdonald et al. 1983, 1984, 1985a, 1985b, 1985c). The extent of such effects can usually be correlated with the bulk and the rigidity of the substituent groups as well as

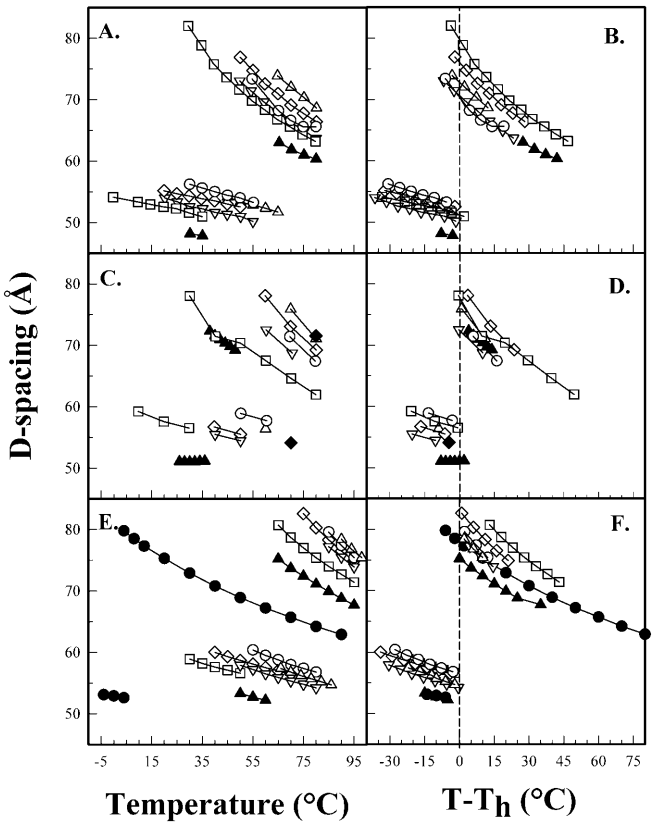

Fig. 6 Unit cell basis vector lengths (Å) versus **A** temperature (°C) for 16-carbon ECL α-D-GlcDAGs, **B** reduced temperature [T–T_h (°C)] for 16-carbon α-D-GlcDAGs, **C** temperature (0 °C) for 18-carbon α-D-GlcDAGs, **D** reduced temperature [T–T_h (°C)] for 18-carbon α-D-GlcDAGs, **E** temperature (0 °C) for 18-carbon PEs (from Harper et al. 2001), **F** reduced temperature [T–T_h (°C)] for 18-carbon PEs. The *d*-spacings at T–T_h (°C) are listed in Table 5. The symbols for each lipid are as follows: *filled circles*: di-*cis*-monounsaturated; *filled triangles*: di-*trans*-monounsaturated; *empty squares*: ethyl-anteiso-branched; *empty diamonds*: dimethyl-iso-branched; *empty triangles*: methyl-iso-branched; *empty inverted triangles*: methyl-anteiso-branched; *empty circles*: ω-cyclohexyl-branched; *filled diamonds*: di-saturated; *empty octagons*: di-*cis*-diunsaturated

their position on the chain. One exception to this rule is glycerolipids with acyl chains containing a terminal cyclohexyl group. In such cases, the cyclohexane ring appears to increase disorder in the gel phase, but increases the order of the liquid-crystalline phase, producing a smaller change in the chain-averaged orientational order of the lipids across the transition relative to those of saturated straight-chain compounds of the same ECL.

The inverse chain length dependence of T_{NL} can be correlated with increases in the cross-sectional area of the melted chains. In the case of the α-D-GlcDAGs studied here, many of the shorter-chain lipids also readily form one or more inverted cubic phases at temperatures below the formation of the H_{II} phase. It has been suggested that these Q_{II} phases may represent a compromise in terms of lipid molecular packing which can be explained in terms of small differences in the monolayer curvature or elastic free energy term of each inverted nonlamellar phase (Turner et al. 1992; Seddon and Templer 1993; Templer et al. 1994, 1995). One contribution towards this curvature free energy term comes from the intrinsic differences in chain packing/volume of the various hydrocarbon chain structures. This seems likely since it has been shown that the addition of *n*-alkanes can relieve the packing stress associated with the formation of an H_{II} phase, effectively lowering the T_h (Kirk et al. 1984; Gruner 1985). However, this does not explain the differences in the distribution of T_m, T_h and $\Delta T_{L/NL}$ on the absolute temperature scale of the PEs and the α-D-GlcDAGs.

A comparison of the T_m, T_h and $\Delta T_{L/NL}$ values for the full range of chain lengths and chain structures in both the PEs and α-D-GlcDAGs is possible using the data listed in Tables 1, 2, 3, 4. The T_m and T_h values of the α-D-GlcDAGs are lower on the absolute temperature scale than those of the PEs, yet cover a similar span of temperatures in each lipid (T_m values: PEs, 54.2 °C; α-D-GlcDAGs, 51.9 °C; T_h values: PEs, 47.2 °C; α-D-GlcDAGs, 44.0 °C). These T_m and T_h values follow a similar order in both the PEs and α-D-GlcDAGs, which is dependent on the hydrocarbon chain structure as follows: saturated straight chain > methyl-iso- > ω-cyclohexyl- > methyl-anteiso- > dimethyl-iso- > *trans*-monounsaturated > ethyl-anteiso-branched. Consequently, the $\Delta T_{L/NL}$ values generally show the same order of dependence on hydrocarbon chain structure in both the PEs and the α-D-GlcDAGs. This strongly suggests that the differences in the hydrocarbon chain structure have a generally similar effect on the L/NL phase properties in both classes of lipids. However, in the PEs the $\Delta T_{L/NL}$ values are generally larger than those of the α-D-GlcDAGs (ranging from 5 to 25 °C in the 18-carbon ECL α-D-GlcDAGs and from 25 to 35 °C in the 18-carbon ECL PEs). Higher values of $\Delta T_{L/NL}$ indicate that the PEs have a smaller propensity to form the H_{II} phase than do the α-D-GlcDAGs with an identical fatty acid composition. At this same ECL, the range of $\Delta T_{L/NL}$ values in the PEs is less than those in the α-D-GlcDAGs (Fig. 4). The narrower range of $\Delta T_{L/NL}$ values in the PEs suggests that the PE headgroup has a greater ability to counteract variations in the packing properties of different hydrocarbon chain structures, such as the hydrocarbon chain cross-sectional area and the chain-averaged orientational order (see the discussion above) than does the α-D-GlcDAG headgroup. This idea is supported by the observation that, over the entire range of chain lengths and structures of both headgroup configurations, the $\Delta T_{L/NL}$ values for the α-D-GlcDAGs with linear, unbranched-chains are significantly smaller than those with branched-chain structures (solid diamonds and solid triangles in Fig. 4). The corresponding values for the PEs are also at the lower end on the range of $\Delta T_{L/NL}$ values, but are not radically different from the PEs with other chain structures.

Figure 4 also shows that in the α-D-GlcDAGs, the $\Delta T_{L/NL}$ values for the straight-chain (solid diamonds) and methyl-iso-branched (open triangles) compounds

fall along roughly parallel straight lines which differ in their *y*-axis intercepts, whereas in the corresponding PEs the straight lines are replaced by two curved, parallel lines. In both cases, the regular increase in $\Delta T_{L/NL}$ with decreasing chain length supports previous observations that shorter chain lengths, and hence smaller bilayer thicknesses, stabilize the L_α phase and thus increase the L_α/H_{II} phase transition temperature. In addition, Fig. 4 suggests that the ability of the PE headgroup to counteract the hydrocarbon chain packing properties increases with decreasing chain length, significantly expanding the temperature interval over which the L_α phase is stable relative to the corresponding regions in the α-D-GlcDAGs.

On the basis of the DSC and X-ray diffraction measurements performed in this study, we have outlined the relationship between these L/NL phase transitions in the saturated straight-chain PEs and α-D-GlcDAGs in terms of a general phase diagram outlining the dependence of these transition temperatures on hydrocarbon chain length (Fig. 7). Increases in chain length increase T_m and decrease T_h, whereas changes in chain structure shift both T_m and T_h to lower temperatures in both the PEs (Fig. 7A) and α-D-GlcDAGs (Fig. 7B) and may also result in small changes in $\Delta T_{L/NL}$, depending on the packing properties of the hydrocarbon chains in the L_β, L_α and H_{II} phases.

The underlying mechanism responsible for differences in the L/NL phase properties of PEs and α-D-GlcDAGs (cf. Fig. 7A and B) containing the same hydrocarbon chain structures is not immediately clear. It is obvious that the molar specific volumes of the branched hydrocarbon chains in the fluid phase are greater than those of the unbranched hydrocarbon chains of comparable length (see tables 1 and 2 of Harper et al. 2001). This is most readily visible in the lipids studied here by a lowering of the T_m. These differences in hydrocarbon chain molar specific volume are determined by a combination of factors including conformational disorder, the efficiency of the hydrocarbon chain packing in the fluid state, and the elastic properties of the chain which determine the average length of the hydrocarbon chains above the T_m. The degree of conformational disorder required to induce the lamellar to inverted nonlamellar phase transition, as well as the rate at which conformational disorder in the liquid-crystalline phase increases with increasing temperature, is likely to differ between compounds containing hydrocarbon chains with different structures and chain lengths (Macdonald et al. 1983, 1984, 1985a, 1985b, 1985c; Lewis et al. 1994). Thus, the relative change in both the length of the chains and cross-sectional area at the methyl terminus as a function of temperature would not be expected to follow the same simple relationship in lipids containing these different hydrocarbon chains. The extent of conformational disorder required to promote the formation of an inverted nonlamellar phase in a lipid bilayer has recently been investigated for some straight-chain lipids using FTIR spectroscopy (Senak et al. 1991; Mendelsohn and Senak 1993), but this has not been extended to branched-chain compounds, nor applied to branched hydrocarbon chains in the bilayer configuration.

Once the hydrocarbon chains are melted, one can infer that this difference between the molar specific volumes of the hydrophobic domains of two lipids with the same headgroup configuration can then exert their effects upon parameters such as intrinsic monolayer curvature and the "preferred shape" of the lipid molecule (however defined).

Headgroup and interfacial regions

From the thermodynamic data presented here for PEs and MGDGs with two hydrocarbon chains, the extent of the involvement of the polar headgroup in the L/NL

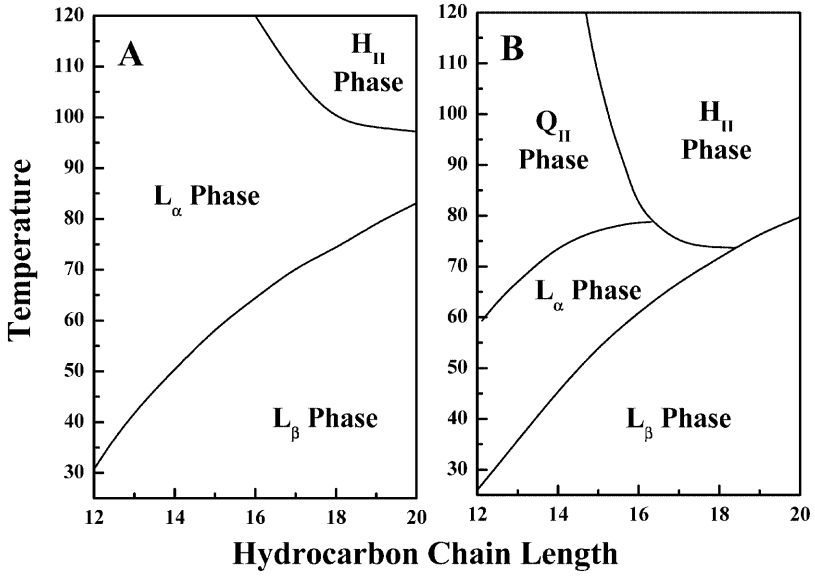

Fig. 7 Generalized phase diagrams illustrating the hydrocarbon chain length dependencies of the lamellar and nonlamellar phase transition temperatures of the saturated straight-chain diacyl PEs (**A**) and α-D-GlcDAGs (**B**)

phase properties in unclear. Recent investigations into the formation of inverted phases in single-chain amphiphiles suggest that both the headgroup and the chains are involved in determining both the lamellar and nonlamellar phase morphologies (Woo et al. 1995; Leitao et al. 1996; Sottmann and Strey 1997, 1998). DSC studies of MGDGs containing two hydrocarbon chains have shown that changing the orientation of the hydroxyl groups around the sugar ring or changing the carbohydrate configuration from a hexopyranoside to a pentopyranoside does not significantly alter T_m but does produce substantial changes the L/NL phase preference (Hinz et al. 1991; Mannock and McElhaney 1991; Mannock et al. 1992; Seddon et al. 1996; Duesing et al. 1997). However, it is not clear from the above measurements exactly what role is played by the headgroup and exactly how it regulates the L/NL phase preference in MGDGs. It is also not clear why the MGDGs tend to form inverted cubic phases readily, whereas PEs with the corresponding acyl chains do not (but see Cantor 1995; Woo et al. 1995).

There are several important contributions to the properties of a lipid polar headgroup including steric effects, headgroup dynamics, hydrogen bonding, hydration and electrostatic interactions. At a simple level, one can view the α-D-GlcDAG headgroup as a bulky, nonionic ring and the PE headgroup as a linear, ionic chain. Differences in the relative increase in headgroup T_1 relaxation and segmental order parameters measured across the L/NL phase transitions in phospho- and glycolipids have been reported and discussed by Jarrell et al. (1987). Increasing the headgroup steric bulk by the addition of one or more methyl groups to the headgroup has different effects in the PEs and MGDGs (Gagne et al. 1985; Trouard et al. 1994). Sequential methylation of PE lowers the T_m and raises the T_h because the addition of a methyl group increases the steric bulk, which weakens the headgroup/headgroup attractive forces and allows more water to penetrate into the interfacial region (Rand and Parsegian 1992, 1997). As a consequence, the tendency of the lipid to form nonbilayer structures decreases. Monomethylation of the β-D-GlcDAlkG also lowers the T_m, yet it also appears to drastically decrease the headgroup and interfacial hydration which, in turn, destabilizes both the L_β and L_α phases and, as a result, the L/NL tendency increases and the T_{NL} is lowered (Trouard et al. 1994). Thus, the same chemical modification of a lipid headgroup can have opposite effects on the L/NL phase preference in different lipid classes. Moreover, chemical modification of the polar headgroup may also involve changes in the polar headgroup hydration. This latter conclusion is supported by observations in which the substitution of D_2O for H_2O in some diacyl PEs lowered the L_α/H_{II} phase transition more than it raised the L_β/L_α phase transition (Epand 1990).

For the moment we can only assume that this variation in lipid phase properties with headgroup structure is a reflection of the ionic nature of the phospholipid interface which stabilizes the lamellar phase relative to the nonlamellar phase (Rand and Parsegian 1997). Lewis and McElhaney (2000) have recently demonstrated that, in mixtures of cationic lipids with various zwitterionic and anionic lipids, the tendency to form nonlamellar phases is greatest when the membrane surface charge approaches neutrality. Whether a similar relationship is responsible for the disparate L/NL behaviour of the PEs and α-D-GlcDAGs cannot be definitively answered at this time. However, when the two lipids have chemically distinct headgroup structures (D-glucose and phosphorylethanolamine), the magnitude and nature of local interactions (coulombic, steric and hydrogen bonding including hydration) must be different and it is probably these headgroup contributions which are responsible for regulating the ability of the respective headgroups to counterbalance the packing properties of the different hydrocarbon chain structures. This view is supported by recent measurements of PE/DGDG bilayers using atomic force microscopy, which show that the PEs possess a long-range electrostatic double-layer force which is absent in the glycolipid (Dufrene et al. 1998 and refs cited therein). The sum total of these events must ultimately determine the free energy of the lamellar and nonlamellar phases in the two glycerolipid headgroup configurations studied here.

X-ray diffraction

In order to examine the relative changes in *d*-spacings independently of the L_α/H_{II} phase transition temperature, T_h, we replotted our X-ray *d*-spacings on a normalized reduced temperature scale (T–T_h; cf. Fig. 6a, c, and e with Fig. 6b, d and f). It is clear from Fig. 6b, d and f that the hydrocarbon chain length and structure significantly alter the dimensions of both the L_α and H_{II} phases in both the PEs and the MGDGs. The magnitude of the *d*-spacings in the L_α phases of the 16- and 18 carbon ECL α-D-GlcDAGs (Fig. 6b, d and f) changes with the structure of the hydrocarbon chains. Lipids containing unbranched acyl chains have consistently smaller spacings than do those that contain branched chains. This suggests that the *d*-spacings are dependent on the hydrocarbon chain-averaged orientational order, which can be correlated with the bulk and the rigidity of the substituent groups (see our earlier discussion). In Fig. 6b, d and f, the lamellar *d*-spacings increase in the following order: *cis*-monounsaturated ≥ *trans*-monounsaturated > methyl-anteiso- ≥ methyl-iso- ≥ linear saturated > dimethyl-iso- > ethyl-anteiso- > ω-cyclohexyl-branched. In the H_{II} phase the *d*-spacing decreases rapidly with increasing temperature (Fig. 6b, d and f). In addition, the *d*-spacings of the H_{II} phases are dependent on chain structure and increase in both the PEs and the α-D-GlcDAGs in the order: *trans*-monounsaturated > *cis*-monounsaturated > methyl-anteiso- ≥ methyl-iso- ≥ ω-cyclohexyl- > dimethyl-iso- > ethyl-anteiso-branched.

However, it is not apparent from the *d*-spacings alone which part of the lipid molecule is responsible for this change in H_{II} dimensions. It is also interesting that the dimensions of the H_{II} phases of the 18-carbon-ECL α-D-GlcDAGs are smaller than are those of the corresponding PEs.

These similarities in the dependence of the H_{II} dimensions on chain structure in the PEs and α-D-GlcDAGs suggest that the mechanism of the L_α/H_{II} phase transition might be regulated primarily by changes in the length of the hydrocarbon chains across the transition in both lipid classes. Fourier reconstruction was used to determine the structural dimensions of the 18-carbon ECL PEs (Harper et al. 2001) from their *d*-spacings (Fig. 6e, f). These measurements were only performed on the PEs because insufficient quantities of the glycolipids were available to perform similar Fourier reconstructions. Moreover, several additional problems arise in obtaining data from these glycolipids using the hydration/swelling method commonly employed in phospholipid structural measurements. Of these, the most difficult to overcome is the poor hydration properties of these MGDGs. Sen et al. (1990) managed to overcome this problem in their measurements of a series of saturated straight-chain α-D-GlcDAGs by increasing the thickness of the bilayer by changing the length of the hydrocarbon chains in order to rebuild the continuous transform from the scattering amplitudes (Adachi 2000). However, in the work of Sen et al. (1990), this methodology was only reliable for lipids containing saturated, straight hydrocarbon chains with chain lengths ranging from 14 to 20 carbon atoms. At shorter chain lengths, it was more difficult to accurately determine the position of the lipid/water interface because the penetration of water molecules into the lipid bilayer shifted the position of the polar/apolar interface relative to that of the electron density minimum at the bilayer centre. In the present study, because changing the hydrocarbon chain structure also altered the density minimum at the bilayer centre, it was not possible to apply the method of Sen and co-workers. Furthermore, the absence of an electron dense phosphorus atom in the glycolipid interface makes it impossible to use the same methods which have been applied to the PEs (Turner and Gruner 1992). The absence of these key characteristics makes the calculation of the lipid/water interface in these MGDGs much more difficult. Indeed, any Fourier reconstructions obtained from the glycolipid chain structure variants would all be unique and would require the application of different and more complex analytical methods.

In the Fourier reconstructions of the 18-carbon ECL PEs, the structural parameters of interest are the unit cell basis vector lengths (*d*), the water thickness (*w* and 2*r*), the average lipid thickness ($<l>$) and the average area per lipid headgroup (*A*). Those structural parameters are defined in Fig. 8 (Harper et al. 2001) and the resulting dimensions, plotted on a reduced temperature scale, are shown in Fig. 9. Comparison of the unit cell basis vector lengths and the water thickness on the reduced temperature scale (Figs. 6f and 9a) shows that the H_{II} phase is not formed at a critical L_α phase bilayer thickness, as we had previously suggested (Lewis et al. 1989). From Fig. 9 it is clear that in the L_α phase the average lipid length (Fig. 9b) decreases with increasing temperature for all hydrocarbon chain structures, while the headgroup area at the lipid/water interface (Fig. 9c) is forced to increase. The thickness of the water layer in the L_α phase gradually decreases and is within 1 Å for all hydrocarbon chain structures at the phase transition. The water layer shrinks at roughly the same rate as the headgroup area expands, implying that the aspect of the headgroup area that sets the water layer spacing varies inversely with headgroup area. At the L_α/H_{II} phase transition, the water layer thickness abruptly increases while the headgroup area shows a dramatic decrease. At the same time, the lipid length shrinks by about 1.5 Å, irrespective of the hydrocarbon chain structure. Above the transition to the H_{II} phase the headgroup area remains constant, while the water-layer thickness decreases with increasing temperature for all chain structures examined. There is also a gradual change in the lipid length with increasing temperature, but the rate of change is the same above and below the transition.

The following picture has been suggested as an explanation for this behaviour (Harper et al. 2001). As the temperature increases in the lamellar phase, *gauche*

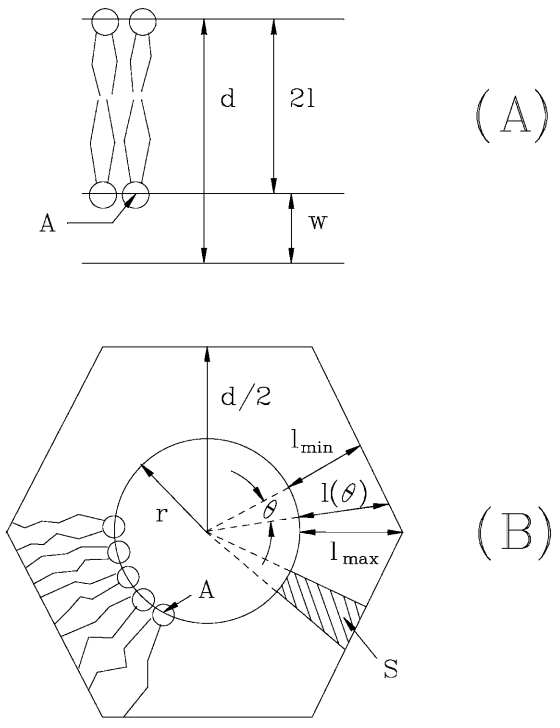

Fig. 8 Typical terminology used in this study to describe **A** the L_α dimensions (*d* is the *d*-spacing, *l* is the lipid length and *w* is the thickness of the water layer between the lipid bilayers) and **B** the H_{II} dimensions (*d* is the *d*-spacing, l_{min} is the minimum lipid length, l_{max} is the maximum lipid length and *r* is the water core radius). Note that, in both diagrams, *A* is the headgroup area at the lipid/water interface and *S* is the area of the hatched region

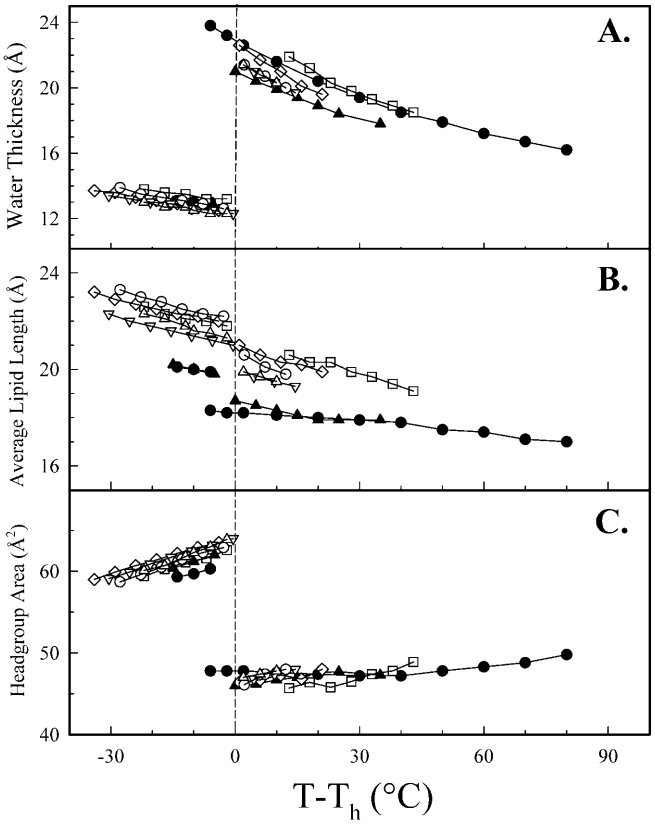

Fig. 9 **A** Water layer thickness versus reduced temperature [T–T_h (°C)]. **B** Average lipid length versus reduced temperature [T–T_h (°C)]. **C** Headgroup area at the lipid/water interface versus reduced temperature [T–T_h (°C)] for the 18-carbon ECL PEs. Values of w (or r), $<l>$ and A at T–T_h (°C) are listed in Table 5. The symbols for each lipid are as follows: *filled circles*: 18:1*c*Δ9-PE; *filled triangles*: 18:1*t*Δ9-PE; *empty squares*: $20{:}0_{eai}$-PE; *empty diamonds*: $20{:}0_{dmi}$-PE; *empty triangles*: 19_i-PE; *empty inverted triangles*: 19_{ai}-PE; *empty circles*: $21{:}0_{ch}$-PE. Note that in the H_{II} phase the headgroup area was constant to within the error bars of these measurements

rotamers are excited in the chains, resulting in a gradual decrease in the lipid length. With this decrease in length comes a concomitant increase in the area per molecule at the lipid/water interface as the hydrocarbon chains splay outward. At a nearly constant volume per lipid molecule, the one-dimensional geometry of the lamellar phase has only one degree of freedom, so a reduction in the lipid thickness necessarily results in an increase in the area per headgroup. At the L_α/H_{II} phase transition, the energetic cost of maintaining this increase in the headgroup area becomes too great and the system is forced to adopt the H_{II} phase. Since the two-dimensional geometry of the H_{II} phase has two degrees of freedom, the lipid monolayer thickness can change independently of the area per lipid headgroup and thus the lipid chains and headgroups are allowed to assume their respective desired states. The fact that the headgroup area in the H_{II} phase does not depend on the hydrocarbon chain structure is clearly shown in Fig. 9c. This in turn suggests that the unfavorable change in lipid headgroup area, enforced by the change in the lipid layer thickness in the lamellar phase, may be viewed as driving the phase transition (Tate and Gruner 1989).

To test the hypothesis that there is a desired headgroup area for a given headgroup in the PEs and α-D-GlcDAGs, we developed a simple model. The purpose of this model was not to provide an elaborate and complete description of all of the physical forces responsible for L/NL phase transitions, but to model the new perspective suggested by our data. This simple model assumes that a component of the system free energy is minimized when the headgroup area, A, is equal to some desired area A_0. The simplest mathematical form for such an energy is $F_A = \alpha((A - A_0)/A_0)^2$, where α is a constant. In the H_{II} phase there is a packing energy, as described in Gruner (1992), which arises from disorder in the hydrocarbon chains and, therefore, is probably entropic in nature, so it would be temperature dependent. The simplest form for such a dependence is $F_P = \beta T$, where β is a constant and T is the absolute temperature (Kelvin). If we assume that packing energy considerations in the lamellar phase are negligible and that headgroup area changes in the hexagonal phase are negligible (e.g., see Gruner 1992), then at the phase transition one expects $F_A = F_P$, i.e.,

Table 6 A comparison of the calculated and measured L_α/H_{II} phase transition temperatures for the PEs and α-D-GlcDAGs containing 18-carbon effective chain length acyl chains. The headgroup area used for the glycolipid calculations was 45.4 Å^2

Lipid	Transition temperatures (°C)		
PE	Measured	Calculated	Difference
18:1*c*Δ9	10.0	21	+11
18:1*t*Δ9	65.0	69	+4
$20{:}0_{eai}$	52.0	53	+1
$20{:}0_{dmi}$	74.0	70	–4
$19{:}0_{ai}$	80.5	78	–2.5
$19{:}0_{i}$	88.0	87	–1
$21{:}0_{ch}$	82.8	85	+2.2
α-D-Glc	Measured	Calculated	Difference
18:1*t*Δ9	34.0	50	+16
$20{:}0_{eai}$	30.5	34	+3.5
$20{:}0_{dmi}$	56.4	48	–8.4
$19{:}0_{ai}$	60.5	59	–1.5
$19{:}0_{i}$	69.0	70	+1
$21{:}0_{ch}$	63.6	67	+3.4

$\beta T = \alpha((A - A_0)/A_0)^2$. Rearranging yields $\alpha/\beta = T/(A - A_0/A_0)^2$. We may use the data in Fig. 9c and Tables 3, 4, 5 to find A and T in the L_α phase and A_0 in the H_{II} phase at the L_α/H_{II} phase boundary. The average value of the packing parameter is about $\alpha/\beta = 3000$ (K) for the average desired headgroup area of $A_0 = 47.5$ Å^2. As a check on the accuracy, if we reverse the process by setting $\alpha/\beta = 3000$ and $A_0 = 47.5$ Å^2 and calculate where the L_α/H_{II} phase transition temperature, T, for the PEs in terms of the measured values of A at the L_α/H_{II} phase boundary, we get calculated T values which are within error (5–10 °C, see Table 6).

For comparative purposes, if we assume that the headgroup area in the L_α phase of the corresponding α-D-GlcDAGs is set by the chains and that the ratio of constants is the same (i.e., $\alpha/\beta = 3000$), then the only difference is the desired headgroup area, A_0. From our previously published phase diagram of the di-dodecyl-β-D-Glc-*rac*-glycerol (Turner et al. 1992), we have a corresponding headgroup area, $A_0 = 45.4$ Å^2. The data calculated from this reverse application appear in Table 6 and show excellent agreement with the observed L_α/H_{II} phase transition temperatures in four out of the six α-D-GlcDAGs. This suggests, but by no means proves, that the general mechanism of the L/NL phase transition is the same in both lipids, despite the obvious differences in the chemical configuration of their headgroups.

The crude mathematical model presented here must only be considered as preliminary and not as a definitive analysis of the L/NL phase transition. Despite the absence of complex variables describing the various headgroup and hydrocarbon chain interactions, which are often evident in a theoretical treatment of the L_α/H_{II} phase transition event, this empirically derived analysis seems to have some merit. It should be noted that similar functional forms for the free energy have been independently developed (Marsh 1996a, 1996b), though important contrasts exist. For instance, this model considers the lateral elastic strain to be primarily localized in the headgroup region, while Marsh distributes it throughout a given monolayer. As a first approximation of the structural parameters involved in driving the L_α/H_{II} phase transition, the model presented here suggests that those same parameters determine the transition to the H_{II} phase in both the PEs and the α-D-GlcDAGs. Such an explanation would certainly explain the differences in the nonlamellar phase preference in the various hexopyranoside and pentopyranoside diacyl- and dialkylglycerols which have been investigated to date (Hinz et al. 1991; Mannock and McElhaney 1991; Mannock et al. 1992; Seddon et al. 1996; Duesing et al. 1997).

Acknowledgements This work was supported by operating and major equipment grants from the Canadian Institutes of Health Research (R.N.M.), the Alberta Heritage Foundation for Medical Research (R.N.M.), National Institutes of Health grant GM32614 (S.M.G.) and a Department of Energy grant (DE-FG02-97ER14805) (S.M.G.). D.A.M. was funded by a postdoctoral fellowship from the Alberta Heritage Foundation for Medical Research. D.C.T. was funded by a National Institutes of Health traineeship grant 5T32GM07312 and a New Jersey Garden State Fellowship. P.E.H. gratefully acknowledges fellowship assistance from the National Science Foundation and the Liposome Co. We would also like to thank Onuttom Narayan of the Department of Physics, Princeton University, for his technical assistance in making some of these measurements.

References

Adachi T (2000) A new method for determining the phase in the X-ray diffraction structure analysis of phosphatidylcholine/alcohol. Chem Phys Lipids 107:93–97

Asgharian B, Rice DK, Cadenhead DA, Lewis RNAH, McElhaney RN (1989) The monomolecular film behavior of a homologous series of 1,2-bis(ω-cyclohexylacyl)phosphatidylcholines at the air/water interface. Langmuir 5:30–34

Asgharian B, Cadenhead DA, Mannock DA, McElhaney RN (2000) A comparative monolayer film behaviour study of monoglucosyl diacylglycerols containing linear, methyl-iso- and ω-cyclohexyl fatty acids. Langmuir 16:7315–7317

Balthasar DM, Cadenhead DA, Lewis RNAH, McElhaney RN (1988) The monomolecular film behavior of methyl anteiso-branched chain phosphatidylcholines. Langmuir 4:180–186

Caffrey M (1993) LIPIDAT. A database of thermodynamic data and associated information on lipid mesomorphic and polymorphic transitions. CRC Press, Boca Raton

Cantor RS (1995) The stability of bicontinuous microemulsions: a molecular theory of the bending elastic properties of monolayers comprised of ionic surfactants and nonionic cosurfactants. J Chem Phys 103:4765–4783

Cullis PR, de Kruijff B (1978) The polymorphic phase behaviour of phosphatidylethanolamines of natural and synthetic origin: a ^{31}P-NMR study. Biochim Biophys Acta 513:31–42

Dekker CJ, Geurts van Kessel WSM, Klomp JPG, Pieters J, de Kruiff B (1983) Synthesis and polymorphic behaviour of polyunsaturated phosphatidylcholines and phosphatidylethanolamines. Chem Phys Lipids 33:93–106

Duesing PM, Seddon JM, Templer RH, Mannock DA (1997) Pressure effects on lamellar and inverse curved phases of fully hydrated dialkyl phosphatidylethanolamines and β-D-xylopyranosyl-*sn*-glycerols. Langmuir 13:2655–2664

Dufrene YF, Boland T, Schneider JW, Barger WR, Lee GU (1998) Characterization of the physical properties of model biomembranes at the nanometer scale with the atomic force microscope. Faraday Discuss 111:79–94

Epand RM (1990) Hydrogen bonding and the thermotropic transitions of phosphatidylethanolamines. Chem Phys Lipids 52:227–230

Gagne J, Stamatatos L, Diacovo T, Hui SW, Yeagle PL, Silvius JR (1985) Physical properties and surface interactions of bilayer membranes containing *N*-methylphosphatidylethanolamine. Biochemistry 24:4400–4408

Gruner SM (1985) Curvature hypothesis: does intrinsic curvature determine biomembrane lipid composition. A role for non-bilayer lipids. Proc Natl Acad Sci USA 82:3665–3669

Gruner SM (1992) Nonlamellar lipid phases. In: Yeagle PL (ed) The structure of biological membranes. CRC Press, Boca Raton, pp 211–250

Gruner SM (1994) Coupling between bilayer curvature elasticity and membrane protein activity. In: Blank M, Vodyanoy I (eds) Biomembrane electrochemistry. (Advances in chemistry series, vol 235) American Chemical Society, Washington, pp 129–149

Harper PE, Gruner SM, Lewis RNAH, McElhaney RN (1993) Structural and free energy investigations into the L_α/H_{II} transition for PE lipids with 18 carbon effective chain length tails. Biophys J 64:A71

Harper PE, Mannock DA, Lewis RNAH, McElhaney RN, Gruner SM (2001) X-ray determination and comparison of the molecular structure of some phosphatidylethanolamines in

the lamellar and inverse hexagonal (H_{II}) phases. Biophys J (in press)

Hinz H-J, Kuttenreich H, Meyer R, Renner M, Fründ R (1991) Stereochemistry and size of sugar headgroups determine the structure and phase behavior of glucolipid membranes. Densitometric, calorimetric and X-ray studies. Biochemistry 30:5125–5138

Ishizuka I, Yamakawa T (1985) Glycoglycerolipids. In: Wiegandt H (ed) Glycolipids. Elsevier, Amsterdam, pp 101–197

Israelachvilli JN, Mitchell DJ, Ninham BW (1977) Theory of self-assembly of lipid bilayers and vesicles. Biochim Biophys Acta 470:185–201

Israelachvilli JN, Marcelja S, Horn RG (1980) Physical principles of membrane organization. Q Rev Biophys 13:121–200

Jarrell HC, Wand AJ, Giziewicz JB, Smith ICP (1987) The dependence of glycerolipid orientation and dynamics on headgroup structure. Biochim Biophys Acta 897:69–82

Kirk GL, Gruner SM, Steim DL (1984) A thermodynamic model of the lamellar (L_α) to inverse hexagonal (H_{II}) phase transition of lipid membrane-water systems. Biochemistry 23:1093–1102

Leitao H, Somoza AM, Dagama MMT, Sottmann T, Strey R (1996) Scaling of the interfacial tension of microemulsions: a phenomenological description. J Chem Phys 105:2875–2883

Lewis RNAH, McElhaney RN (1992) The mesomorphic phase behavior of lipid bilayers. In: Yeagle PL (ed) The structure of biological membranes. CRC Press, Boca Raton, pp 73–155

Lewis RNAH, McElhaney RN (1993) Calorimetric and spectroscopic studies of the polymorphic phase behavior of a homologous series of n-saturated 1,2-diacylphosphatidylethanolamines. Biophys J 64:1081–1096

Lewis RNAH, McElhaney RN (2000) Surface charge markedly attenuates the nonlamellar phase-forming propensities of lipid bilayer membranes: calorimetric and ^{31}P-nuclear magnetic resonance studies of mixtures of cationic, anionic, and zwitterionic lipids. Biophys J 79:1455–1464

Lewis RNAH, Mannock DA, McElhaney RN, Turner DC, Gruner SM (1989) Effect of fatty acid chain length and structure on the lamellar gel to liquid-crystalline and lamellar to reversed hexagonal phase transitions of aqueous phosphatidylethanolamine dispersions. Biochemistry 28:541–548

Lewis RNAH, Mannock DA, McElhaney RN (1990a) Lamellar to nonlamellar phase transitions of phosphatidylethanolamines and monoglycosyl diacylglycerols. Zbl Bakt Suppl 20:643–645

Lewis RNAH, Mannock DA, McElhaney RN, Wong PTT, Mantsch HH (1990b) The physical properties of glycosyl diacylglycerols. An infrared spectroscopic study of the gel phase polymorphism of the 1,2-di-*O*-acyl-3-*O*-(β-D-glucopyranosyl)-*sn*-glycerols. Biochemistry 29:8933–8943

Lewis RNAH, McElhaney RN, Harper PE, Turner DC, Gruner SM (1994) Studies of the thermotropic phase behavior of phosphatidylcholines containing 2-alkyl substituted fatty acyl chains: a new class of phosphatidylcholines forming inverted nonlamellar phases. Biophys J 66:1088–1103

Lewis RNAH, Mannock DA, McElhaney RN (1997) Membrane lipid molecular structure and polymorphism. In: Epand RM (ed) Lipid polymorphism and membrane properties. Curr Top Membr 44:25–102

Macdonald PM, McDonough B, Sykes BD, McElhaney RN (1983) ^{19}F-nuclear magnetic resonance studies of lipid fatty acyl chain order and dynamics in *Acholeplasma laidlawii* B membranes. The effects of methyl-branch substitution and of *trans*-unsaturation upon membrane acyl chain orientational order. Biochemistry 22:5103–5111

Macdonald PM, Sykes BD, McElhaney RN (1984) Fatty acyl chain structure and the lipid phase transition in *Acholeplasma laidlawii* B membranes. A review of recent ^{19}F nuclear magnetic resonance studies. Can J Biochem Cell Biol 62:1134–1150

Macdonald PM, Sykes BD, McElhaney RN, Gunstone FD (1985a). ^{19}F-nuclear magnetic resonance studies of lipid fatty acyl chain order and dynamics in *Acholeplasma laidlawii* B membranes. Orientational order in the presence of a series of positional isomers of *cis*-octadecenoic acid. Biochemistry 24:177–184

Macdonald PM, Sykes BD, McElhaney RN (1985b) ^{19}F-nuclear magnetic resonance studies of lipid fatty acyl chain order and dynamics in *Acholeplasma laidlawii* B membranes. Orientational order in the presence of positional isomers of *trans*-octadecenoic acid. Biochemistry 24:2237–2245

Macdonald PM, Sykes BD, McElhaney RN (1985c) ^{19}F nuclear magnetic resonance studies of lipid fatty acyl chain order and dynamics in *Acholeplasma laidlawii* B membranes. A direct comparison of the effects of *cis*- and *trans*-cyclopropane ring and double-bond substituents on orientational order. Biochemistry 24:4651–4659

Mannock DA, McElhaney RN (1991) Differential scanning calorimetry and X-ray diffraction studies of a series of synthetic β-D-galactosyl diacylglycerols. Biochem Cell Biol 69:863–867

Mannock DA, Lewis RNAH, Sen A, McEhaney RN (1988) Physical properties of glycosyldiacylglycerols. Calorimetric studies of a homologous series of 1,2-di-*O*-acyl-3-*O*-(β-D-glucopyranosyl)-*sn*-glycerols. Biochemistry 27:6852–6859

Mannock DA, Lewis RNAH, McElhaney RN (1990a) Physical properties of glycosyl diacylglycerols. 1. Calorimetric studies of a homologous series of 1,2-di-*O*-acyl-3-*O*-(α-D-glucopyranosyl)-*sn*-glycerols. Biochemistry 29:7790–7799

Mannock DA, Lewis RNAH, McElhaney RN (1990b) The chemical synthesis and physical characterization of 1,2-di-*O*-acyl-3-*O*-(α-D-glucopyranosyl)-*sn*-glycerols: an important class of membrane glycolipids. Chem Phys Lipids 55:309–321

Mannock DA, Lewis RNAH, McElhaney RN, Akiyama M, Yamada H, Turner DC, Gruner SM (1992) Effect of the chirality of the glycerol backbone on the bilayer and nonbilayer phase transitions in the diastereomers of didodecyl-β-D-glucopyranosyl glycerol. Biophys J 63:1355–1368

Mannock DA, Akiyama M, Lewis RNAH, McElhaney RN (2000) Synthesis and thermotropic phase properties of an homologous series of racemic β-D-glucosyl dialkylglycerols. Biochim Biophys Acta 1509:203–215

Mannock DA, Harper PE, Gruner SM, McElhaney RN (2001) The physical properties of glycosyl diacylglycerols. Calorimetric, X-ray diffraction and Fourier transform infrared spectroscopic studies of a homologous series of 1,2-di-*O*-acyl-3-*O*-(β-D-galactopyranosyl)-*sn*-glycerols. Chem Phys Lipids 111:139–161

Marsh D (1990). Handbook of lipid bilayers. CRC Press, Boca Raton

Marsh D (1991) Analysis of the chain length dependence of lipid phase transition temperatures: main and pretransitions of phosphatidylcholines; main and nonlamellar transitions of phosphatidylethanolamines. Biochim Biophys Acta 1062:1–6

Marsh D (1996a) Components of the lateral pressure in lipid bilayers deduced from H_{II} phase. Biochim Biophys Acta 1279:119–123

Marsh D (1996b) Intrinsic curvature in normal and inverted lipid structures and in membranes. Biophys J 70:2248–2255

Mendelsohn R, Senak L (1993) Quantitative determination of conformational disorder in biological membranes by FTIR spectroscopy. In: Clark RJH, Hester RE (eds) Biomolecular spectroscopy. (Advances in spectroscopy, vol 21) Wiley, New York, pp 339–380

Monck MA, Bloom M, Lafleur M, Lewis RNAH, McElhaney RN, Cullis PR (1992) Influence of lipid composition on the orientational order in *Acholeplasma laidlawii* strain B membranes: a deuterium NMR study. Biochemistry 31:10037–10043

Nagle JF, Wilkinson DA (1978) Lecithin bilayers: density measurements and molecular interactions. Biophys J 23:159–175

Rand RP, Parsegian VA (1992) The forces between interacting bilayer membranes and the hydration of phospholipid assemblies. In: Yeagle PL (ed) Structure of biological membranes. CRC Press, Boca Raton, pp 73–155

Rand RP, Parsegian VA (1997) Hydration, curvature and bending elasticity of phospholipid monolayers. In: Epand RM (ed) Lipid polymorphism and membrane properties. Curr Top Membr 44:167–189

Reynolds GT, Milch JR, Gruner SM (1978) A high sensitivity intensifier-TV detector for X-ray diffraction studies. Rev Sci Instr 49:1241–1249

Rice DK, Cadenhead DA, Lewis RNAH, McElhaney RN (1987) A comparative monomolecular film study of a straight-chain phosphatidylcholine (dipalmitoylphosphatidylcholine) with three isobranched-chain phosphatidylcholines (diisoheptadecanoyl phosphatidylcholine, diisooctadecanoyl phosphatidylcholine, and diisoeicosanoyl phosphatidylcholine). Biochemistry 26:3205–3210

Seddon JM, Templer RH (1993) Cubic phases of self-assembled amphiphilic aggregates. Phil Trans Roy Soc A 344:377–401

Seddon JM, Cevc G, Marsh D (1983) Calorimetric studies of the gel-fluid (L_β-L_α) and lamellar-inverted hexagonal (L_α-H_{II}) phase transitions in dialkyl- and diacylphosphatidylethanolamines. Biochemistry 22:1280–1289

Seddon JM, Cevc G, Kaye RD, Marsh D (1984) X-ray diffraction study of the polymorphism of hydrated dialkyl- and diacylphosphatidylethanolamines. Biochemistry 23:2634–2644

Seddon JM, Hogan JL, Warrender NA, Pebay-Peroula E (1990) Structural studies of phospholipid cubic phases. Prog Colloid Polym Sci 81:189–197

Seddon JM, Zeb N, Templer RH, McElhaney RN, Mannock DA (1996) An *Fd3m* lyotropic cubic phase in a binary glycolipid/water system Langmuir 12:5250–5253

Sen A, Hui S-W, Mannock DA, Lewis RNAH, McElhaney RN (1990) Physical properties of glycosyldiacylglycerols. X-ray diffraction studies of a homologous series of 1,2-di-*O*-acyl-3-*O*-(α-D-glucopyranosyl)-*sn*-glycerols. Biochemistry 29:7799–7804

Senak L, Davies MA, Mendelsohn R (1991) A quantitative IR study of hydrocarbon chain conformation in alkanes and phospholipids: CH_2 wagging modes in disordered bilayer and H_{II} phases. J Phys Chem 95:2565–2571

Silvius JR, McElhaney RN (1978) Lipid compositional manipulation in *Acholeplasma laidlawii* B. Effect of exogenous fatty acids on fatty acid composition and cell growth when endogenous fatty acid production is inhibited. Can J Biochem 56:462–469

Sottmann T, Strey R (1997) Ultralow interfacial tensions in water n-alkane surfactant systems. J Chem Phys 106:8606–8615

Sottmann T, Strey R (1998) Structures and interface tensions in microemulsions. Tens Surfact Deterg 35:34–45

Tate MW, Gruner SM (1989) Temperature dependence of the structural dimensions of the inverted hexagonal (H_{II}) phase of phosphatidylethanolamine containing membranes. Biochemistry 28:4245–4253

Tate MW, Shyamsunder E, Gruner SM, D'Amico KL (1992) Kinetics of the lamellar-hexagonal phase transition determined by time-resolved X-ray diffraction. Biochemistry 31:1081–1092

Tate MW, Gruner SM, Eikenberry EF (1997) Coupling format variations in X-ray detectors based on charge coupled devices. Rev Sci Instr 68:47–54

Templer RH, Seddon JM, Warrender NA (1994) Measuring the elastic parameters for inverse bicontinuous cubic phases. Biophys Chem 49:1–12

Templer RH, Turner DC, Harper PE, Seddon JM (1995) Corrections to some models of the curvature elastic energy of inverse bicontinuous cubic phases. J Phys II Fr 5:1053–1065

Trouard TP, Mannock DA, Lindblom G, Rilfors L, Akiyama M, McElhaney RN (1994) Thermotropic phase properties of 1,2-di-*O*-tetradecyl-3-*O*-(3-*O*-methyl-β-D-glucopyranosyl)-*sn*-glycerol. Biophys J 67:1090–1100

Turner DC, Gruner SM (1992) X-ray diffraction reconstruction of the inverted hexagonal (H_{II}) phase in lipid-water systems. Biochemistry 31:1340–1355

Turner DC, Wang Z-G, Gruner SM, Mannock DA, McElhaney RN (1992) Structural study of the inverted cubic phases of didodecyl-β-D-glucopyranosyl-*rac*-glycerol. J Phys II France 2:2039–2063

Woo HJ, Carraro C, Chandler D (1995) Quantitative molecular interpretation of mesoscopic correlations in bicontinuous microemulsions. Phys Rev E 52B:6497–6507